# STUDY OF EXCITATION TRANSFER IN A FLOWING HELIUM AFTERGLOW PUMPED WITH A TUNEABLE DYE LASER

## II. Measurement of the Rate Coefficient for the Rotational Relaxation of $He_2(3p\,^3\Pi g)$



by

C. B. Collins and B. W. Johnson

The University of Texas at Dallas
Dallas, Texas 75230

Research supported by the Atmospheric and Space Sciences, National Aeronautics and Space Administration, NASA Grant NGL44-004-001.

SP-72-006-II.

## ABSTRACT

The rotational relaxation of the $He_2(3p^3\Pi g)$ state is examined by optically pumping a flowing helium afterglow with a tuneable dye laser. The population of the J = 8 rotational state is enhanced by optically saturating the $R_7$ component of the transition connecting this state with the metastable $He_2(2s^3\Sigma_u^+)$ molecular state. From the lifetime and yield of the $Q_7$ component, the rate coefficient for the rotational relaxation via the forbidden $\Delta J = 1$ channel is determined to be of the order of $2 \times 10^{-11}$ $cm^3/sec$. It is found that this represents about half of the total rate of rotational relaxation in this state.

# INTRODUCTION

The previous paper[1] describes a system and technique of fluorescent spectroscopy which is suitable for the study of excitation quenching reactions of species with lifetimes in the nanosecond range. In that system use is made of a two-step excitation process in which a tuneable laser optically pumps a stationary population of metastable species in a flowing afterglow. Because of the narrow spectral width of the continuously tuneable laser output, such a system offers the possibility of enhancing the population of single rotational levels of excited molecular states. From such a selectively excited afterglow, direct information about the rate of rotational relaxation can be obtained from subsequent examination of the resulting fluorescence.

This paper reports the results of the use of this fast-transient fluorescence technique in the examination of rotational relaxation caused by collisions with neutral helium atoms of the $He_2(3p\,^3\Pi g)$ state. Although overall rates of rotational relaxation are well-known for ground state molecules[2], there is little corresponding information for such electronically excited states. While the gross rates for de-excitation are expected to be similar, it is conceivable that selection rules on particular reaction channels for rotational relaxation might be less rigorous as a consequence of the greater abundance of diabatic states for the higher levels.

In these experiments, particular emphasis was placed upon the $\Delta J = 1$ relaxation channel which is forbidden for homonuclear molecules in first order theory[3]. In contrast to that theory, it is reported here that for this particular electronic state the $\Delta J = 1$ channel was found to account for about half of the total relaxation rate.

## METHODS

### A. Production and Detection of Reacting Species

The enhanced population of the $3p^3\Pi g$ state of molecular helium was produced by optically pumping the primary population of $He_2(2s^3\Sigma_u^+)$ metastable state according to the scheme

$$He_2(2s^3\Sigma_u^+) + h\nu(\text{nom. } 4650\text{Å}) \rightarrow He_2(3p^3\Pi g) \quad . \quad (1)$$

Figure 1 shows a diagram of the corresponding energy levels for the equilibrium internuclear separation of the molecular states involved in this experiment. Energies are shown in $cm^{-1}$ relative to the lowest rotational level of the molecular metastable state. Integers denote the rotational quantum number, J. Only the rotational levels of the vibrationless state of each of the two electronic configurations are shown as the vibrationally excited states are only weakly populated in the flowing helium afterglow serving as the source of primary species.

Channels for the rotational relaxation through collisions involving the transfer of an odd number of rotational quanta can be readily isolated from those requiring change of an even number by making use of the natural spectral separation of the P, Q and R branches of the radiative transition connecting the levels of two electronic states. Since excitation of the $2s^3\Sigma_u^+ \rightarrow 3p^3\Pi g$ transition is forbidden for branches having even J-numbered rotational levels in the lower state, optical pumping of the spectrally isolated R-branch serves to produce only even-numbered rotational levels of the upper state. Figure 2 illustrates this isolation showing a schematic representation of the dispersed 4560Å band

($2s^3\Sigma_u^+ \rightarrow 3p^3\Pi g$). Optical pumping of the $R_7$ line was selected in this experiment in order to allow about 20Å separation between the laser wavelength and the first component which could spuriously populate an odd-J rotational level of the upper state. This represents about an order of magnitude larger separation than any anomalous system effects due to linewidth or jitter of the pumping wavelength. In practice however, such effects did provide some excitation of the $R_5$ and $R_9$ components which effectively obscured observation of rotational relaxation in the $\Delta J = 2$ channel.

The lifetime of the enhanced population of the upper state was conveniently monitored by observation of the transient fluorescence of the $P_9$ component of the same transition. In this way 55Å separation could be obtained between the wavelength of the $P_9$ transition and any non-resonant scattering of the $R_7$ pumping light from imperfections in the optical windows. This proved more than sufficient to insure that such scattered light was completely rejected by the tandem monochromator used in the detecting system. Figure 1 summarizes the relation of these spectral components on the energy scale.

As can be seen in Figure 1, the enhancement of radiation of the $Q_7$ component can only occur as a consequence of rotational relaxation from some even-J level. Representing the effective reaction connecting the input and output channel, this can be written,

$$He_2(3p^3\Pi g,\ J=8) + He \rightarrow He_2(3p^3\Pi g,\ J=7) + He \quad , \qquad (2)$$

followed by

$$He_2(3p^3\Pi g,\ J=7) \rightarrow He_2(2s^3\Sigma_u^+,\ J=7) + h\nu(Q_7) \quad . \qquad (3)$$

In this case the yield of photons in reaction (3) is a direct measure of the effective rate at which reaction (2) proceeds, recognizing that the actual reaction path may involve intermediate states. However, since only even-numbered J states can be directly or spuriously excited in the upper state when pumping in the R-branch, any assumed intermediate paths must involve an odd change in J which is as forbidden as the direct reaction (2), itself. Consequently, indication of a large effective rate for (2) implies a breakdown of the selection rule requiring $\Delta J$ be even.

## B. Analytical Method

While the total collisional loss rate of the enhanced population can be obtained from the partial derivative of destruction frequency with respect to neutral particle concentration, as was done[1] in part I, the yield of photons in the product channel also give an estimate of the rate coefficient connecting initial and final channels of the reaction. Denoting the enhanced populations of the initial level of the $3p^3\Pi g$ electronic state by $N_i$ and the population of the final level by $N_f$ and assuming both populations are far from equilibrium values,

$$\frac{dN_i}{dt} = -(L_i + S)N_i \quad , \qquad (4)$$

$$\frac{dN_2}{dt} = SN_i - L_fN_f \quad , \qquad (5)$$

where $L_i$ and $L_f$ denote the total loss rates exclusive of the reaction connecting

the initial and final levels, respectively, and S represents the rate of that reaction connecting the levels. Assuming the initial conditions

$$N_i(0) = N \qquad \text{and} \qquad N_f(0) = 0 \quad , \qquad (6)$$

representing an instantaneous increase of initial-state population to N at time t = 0, corresponding to the laser pulse, and solving for the populations gives expressions which can be written in terms of fluorescent intensities through the following substitutions,

$$C_i = f\varepsilon_i{}^b A_i \; S^b_{J_i} (2J_i + 1)^{-1} \int_0^\infty N_i dt \quad , \qquad (7)$$

$$C_f = f\varepsilon_f{}^b A_f \; S^b_{J_f} (2J_f + 1)^{-1} \int_0^\infty N_f dt \quad . \qquad (8)$$

In these expressions C represents the total number of photoelectrons counted during the fluorescent period following a single laser pulse and corresponds to the intensity radiated from the respective population, f represents the collected geometric factors, $\varepsilon$, the photoelectric counting efficiency, A, the part of the spontaneous transition probability not including rotational effects, S the Hönl-London line strength[4]. Subscripted J's denote the rotational quantum number of the level having population N and the superscripted b represents the spectral branch designation, P, Q, or R. Collecting the solutions of (4) and (5) and substituting (7) and (8) gives finally

$$SL_f^{-1} = \frac{C_f}{C_i} \frac{\varepsilon_i^b}{\varepsilon_f^b} \frac{A_i}{A_f} \frac{(2J_f + 1)}{(2J_i + 1)} \frac{S^b_{J_i}}{S^b_{J_f}} \quad . \qquad (9)$$

Measurement of $L_f$ can be made directly from the lifetime of the decay of the fluorescence from the final state, provided this is comparable to the lifetime of the initial state, and $C_i$ and $C_f$ can be determined from the total number of photons collected at wavelengths characteristic of the monitoring transitions from the initial and final states respectively. Direct knowledge of $A_i$ and $A_f$ is not necessary if those transitions occur between the same electronic configurations. In this case, since the monitoring transition of the initial state population is in the P branch of the $3p\,^3\Pi g \rightarrow 2s\,^3\Sigma_u^+$ system, while that of the final state transition is in the Q branch of the same system, $A_i = A_f$ and that ratio cancels.

## RESULTS

The use of -4- methylcoumarin in the dye laser system produced a pumping flux of the order of $10^{16}$ photons/Å/sec in the 4650Å region. The linewidth was held to the order of 5Å through the use of an iris in the resonant cavity in addition to the grating described in the previous paper[1]. Unlike the particular experiment described there, pumping the metastable population with the relatively high flux available at this wavelength was sufficient to saturate the particular transition involved. Power densities were such that, depending upon the particular details of the mode structure in the laser, cooperative phenomena[5] in the fluorescence from the pumped transition had been expected to affect radiative lifetimes. Some evidence of this is seen in Figure 3 in the spiking behavior of the afterglow fluorescence observed at the highest power densities. In Figure 3 the number of photoelectrons counted during the fluorescent period

are plotted to the right as functions of the delay time following initiation of the laser pulse and to the front as functions of useable energy per pulse in the absorption linewidth. The curves at the two larger energies represent the accumulation of counts from 100 repetitions each, the lower energy curve represents the accumulation for 500 repetitions divided by a scale factor of five. As can be seen, the early lifetime of the fluorescence depends strongly upon the peak power in the optical pumping pulse. To avoid this effect pulse energies not in excess of 2.3 μJ were used in the course of the actual measurements.

Figures 4 and 5 show the decay of the fluorescence in the initial and final states respectively. The former monitors the population of the J = 8 level of the $3p\,^3\Pi g$ state while the latter follows the decay of the J = 7 level which cannot be directly excited by pumping from the R branch. Accumulated photoelectron counts have been converted to counting rates by dividing by the accumulated dwell time in each of the counting channels.

Considering only the gross loss rate for molecules in the J = 8 level, the lifetime of approximately 72 nanoseconds obtained from Figure 4 corresponds to a destruction frequency of $1.4 \times 10^7$ $sec^{-1}$. If this were entirely attributed to the collisional relaxation of the rotation at the neutral pressure of 10 Torr present in the afterglow, the corresponding rate coefficient would be $4.3 \times 10^{-11}$ $cm^3 sec^{-1}$.

The rate coefficient to the $\Delta J = 1$ component channel described by eq. (2) can be estimated from the measurements collected in Table 1 of the factors appearing in eq. (9).

Table I. Photon yield factors appearing in equation (9) and necessary to estimate the rate coefficient of reaction (2).

| Level (J) | Photoelectrons (counts) | Efficiency ($10^{-9}$) | $(2J + 1)/S_J^b$ | $SL_f^{-1}$ |
|---|---|---|---|---|
| 8 | 1057 | 9.7 | 8.5 | - |
| 7 | 1386 | 9.7 | 4.0 | 0.62 |

The value of $L_f^{-1}$ can be read from Figure 5 to be approximately 80 nanoseconds. This gives a rate for reaction (2) of

$$S = 7.8 \times 10^6 \text{ sec}^{-1} \quad , \qquad (10)$$

a value which at 10 Torr corresponds to a rate coefficient of

$$R = 2.4 \times 10^{-11} \text{ cm}^3/\text{sec} \quad . \qquad (11)$$

## CONCLUSIONS

The effective reaction path represented by equation (2) connects input and output channels in which the rotational quantum number of the reacting species has been reduced by one. Though formally forbidden in first order collision theory, this reaction has been measured in this work to have an effective rate coefficient of $2.4 \times 10^{-11}$ $\text{cm}^3\text{sec}^{-1}$, a value corresponding to about half of the total rate coefficient for rotational relaxation in the $3p\,^3\Pi g$ electronic configuration of $He_2$. The most probable interpretation of this apparent contradiction is that this selection rule requiring $\Delta J = 2$ is not as rigorous in such a highly

excited electronic state because of the relatively large number of other states of $He_2$ lying within KT of the $3p^3\Pi g$.

It is interesting to note that the collection of statistically significant data is limited at both high and low pumping intensities. In the former case, the use of an excessively intense correlated source appears to cause progressively shorter lifetimes of the enhanced population as the intensity is increased beyond some threshold value. Conversely, the use of a source of insufficient intensity does not produce statistically significant fluorescent signals in a reasonable number of laser pulses. The relatively short operational lifetime of the flash-lamp pumped dye laser systems places a limit of about 1000 pulses on the duration of a experimental measurement. It appears that as nitrogen pumped dye laser systems[6] are beginning to achieve radiancies comparable to those quoted here for the flashlamp system, those devices may eventually offer considerable improvement to such fast reaction studies since their mean time to instability is substantially greater.

REFERENCES

1. C. B. Collins, B. W. Johnson, and M. J. Shaw, J. Chem Phys __, xxx (xxxx).

2. J. B. Hasted, Physics of Atomic Collisions (Butterworths, London, 1964) p. 471.

3. R. Brout, J. Chem. Phys. 22, 934 (1954).

4. G. Herzberg, Spectra of Diatomic Molecules (D. Van Nostrand Co., Inc., New York, 1950) p. 209.

5. F. T. Arecchi, and E. Courtens, Phys. Rev. A2, 1730 (1970).

6. M. J. Shaw, submitted to IEEE Journal of Quantum Electronics, April 1972.

CAPTIONS

Figure 1: Diagram of the energy levels for the equilibrium internuclear separation of the molecular states of $He_2$ involved in this experiment. Energies are shown relative to the lowest level of the metastable $2s^3\Sigma_u^+$ state and integers represent rotational quantum numbers. Arrows indicate the $R_7$ component used in optical pumping, the $P_9$ component used to monitor the pumped population, and the $Q_9$ component radiated from the population resulting from reaction (2).

Figure 2: Schematic representation of the $He_2$ band at 4650Å from the transition ($3p^3\Pi g \rightarrow 2s^3\Sigma_u^+$). Typical intensities observed in emission are plotted as functions of wavelength. The $R_7$, $P_9$, and $Q_7$ components are indicated.

Figure 3: A plot of the number of photoelectrons counted as a function, to the right, of time into the fluorescent period following the laser pulse. Logarithmic coordinates increasing to the front indicate the energy per laser pulse within the absorption linewidth of the $He_2(2s^3\Sigma_u^+)$ metastable molecules.

Figure 4: Logarithmic plot of the decay as a function of time of the enhanced $J = 8$ population of the $3p^3\Pi g$ state of $He_2$ as evidenced by the detected counting rate of the radiation from the $P_9$ component of the transition indicated. Also shown are error limits corresponding to $\pm$ one standard deviation of the counting rate. The exponential fit to the decay corresponds to a lifetime of 72 nanoseconds.

Figure 5: Logarithmic plot of the decay as a function of time of the enhanced $J = 7$ population of the $3p\,^3\Pi g$ state of $He_2$ resulting from reaction (2). Ordinates give the detected counting rate of the radiation from the $Q_7$ component of the indicated transition from this state. Also shown are error limits corresponding to $\pm$ one standard deviation of the counting rate. The exponential fit to the decay corresponds to a lifetime of 80 nanoseconds.

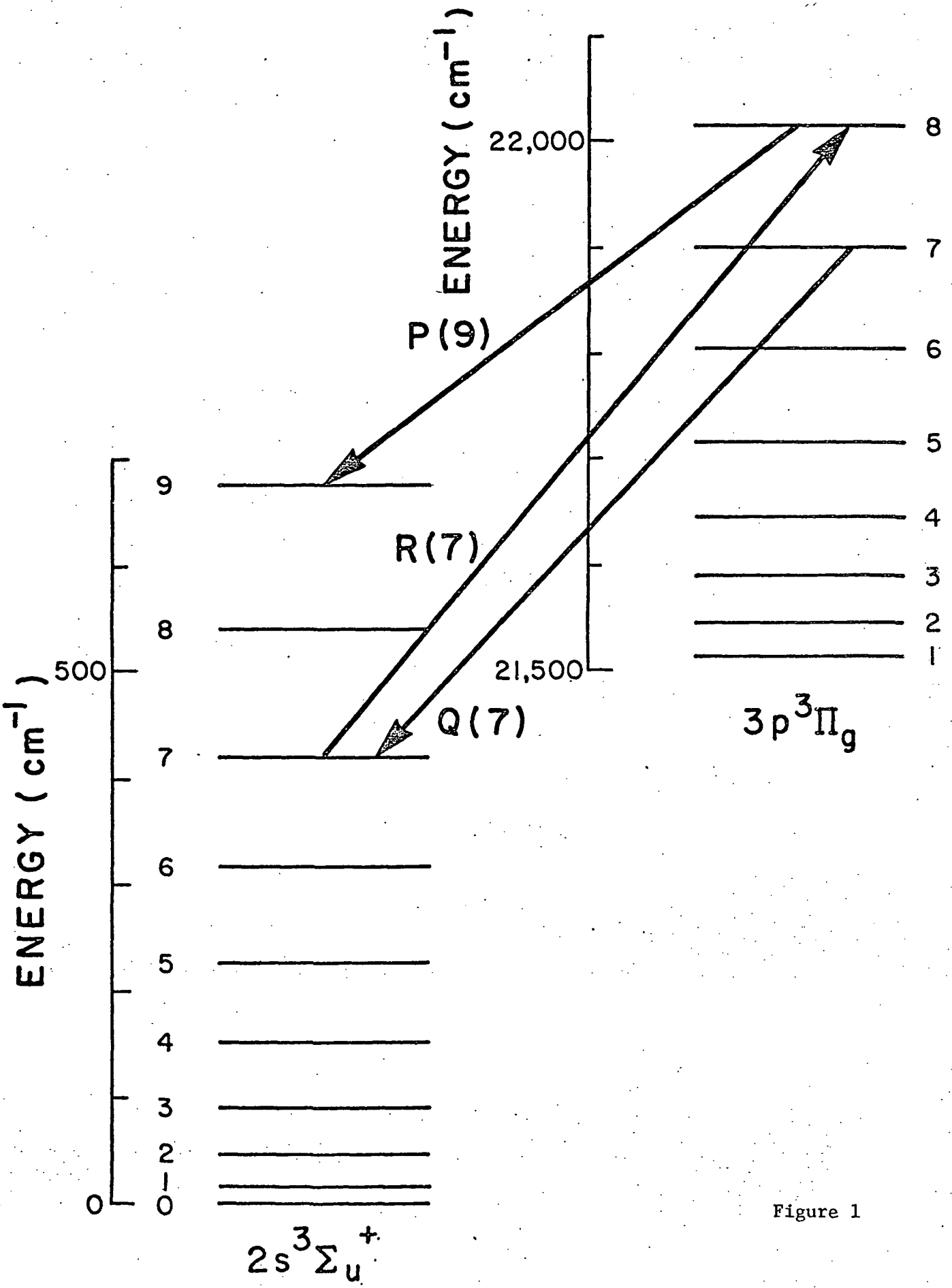


Figure 1

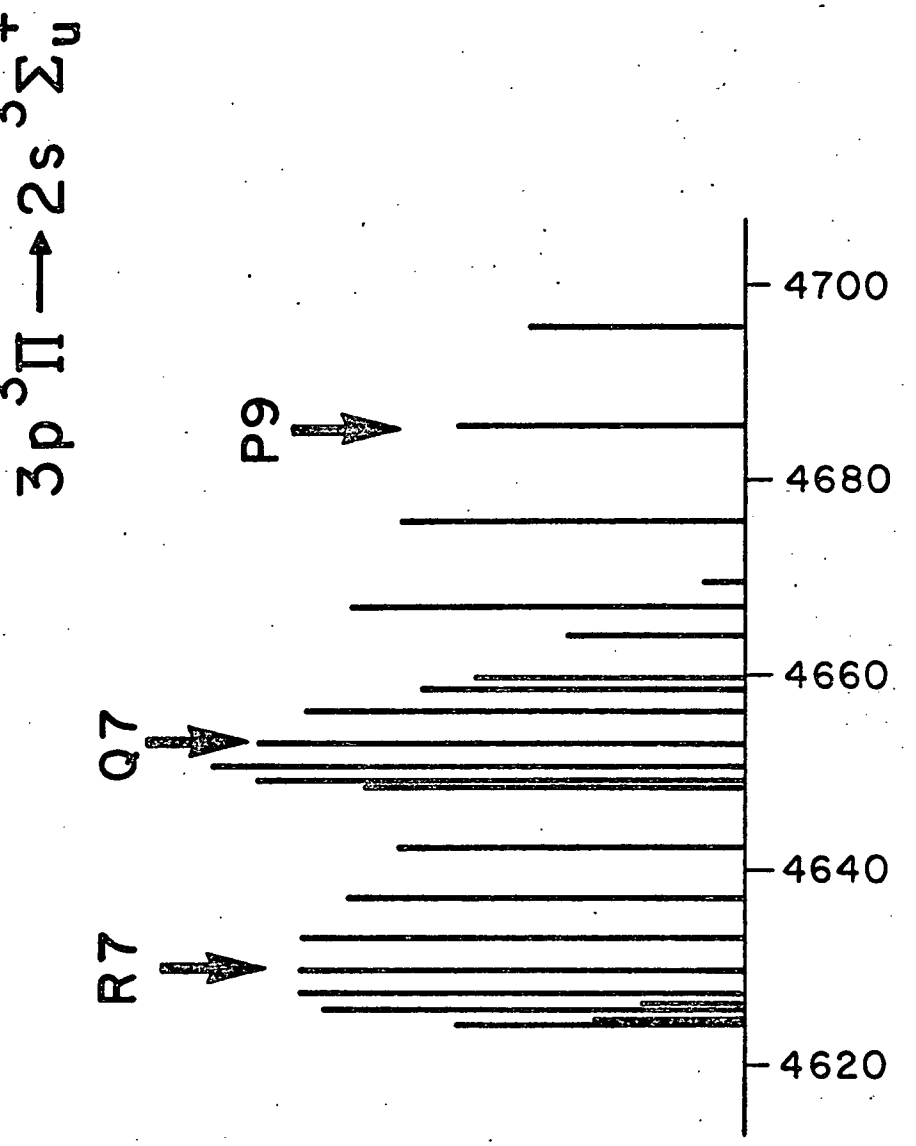
$3p\,^3\Pi \longrightarrow 2s\,^3\Sigma_u^+$
P9
Q7
R7
4700
4680
4660
4640
4620

Figure 2

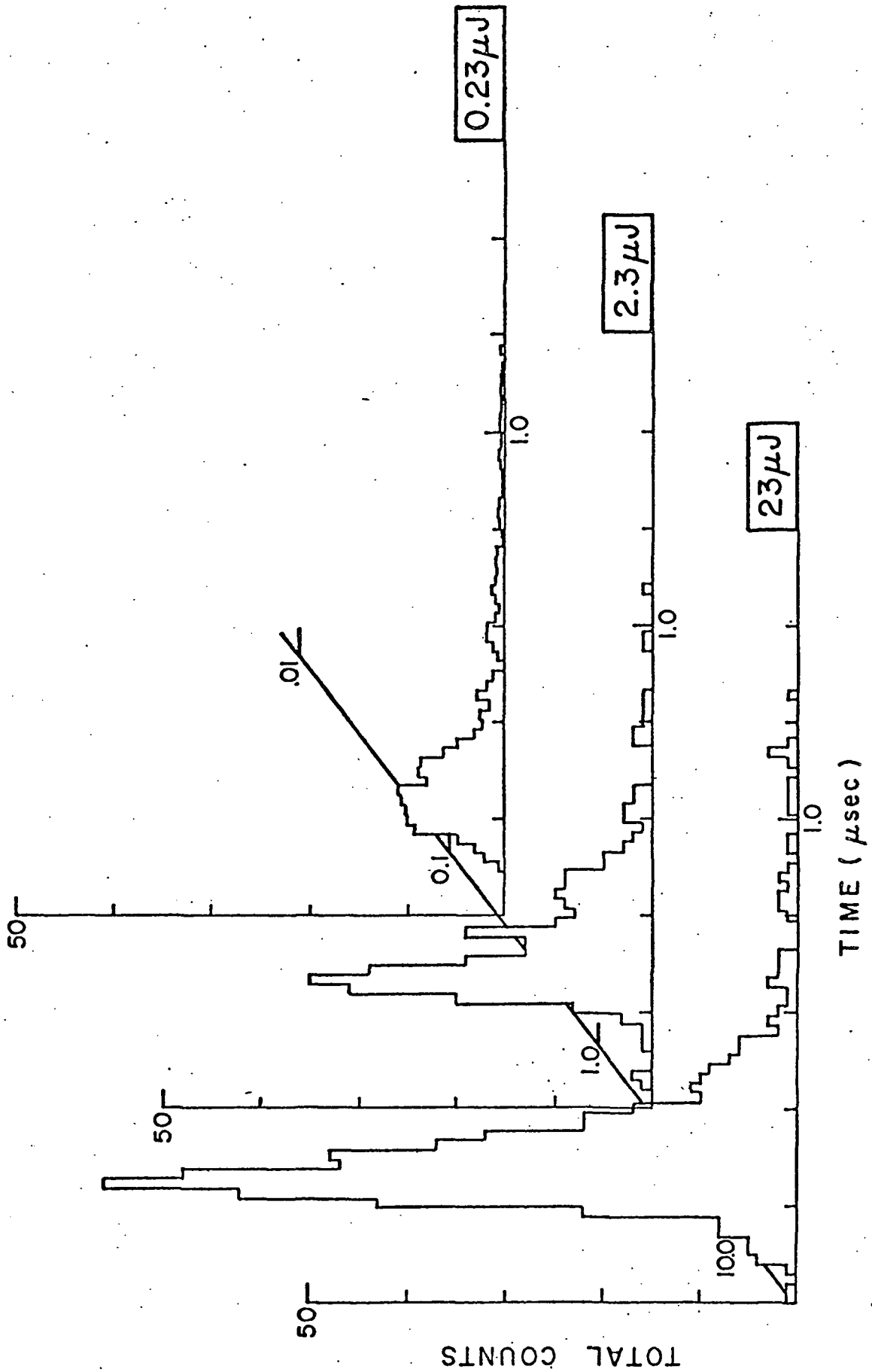
0.23μJ
2.3μJ
23μJ
1.0
.01
.1
1.0
1.0
50
50
50
10.0
TOTAL COUNTS
TIME ( μsec )

Figure 3

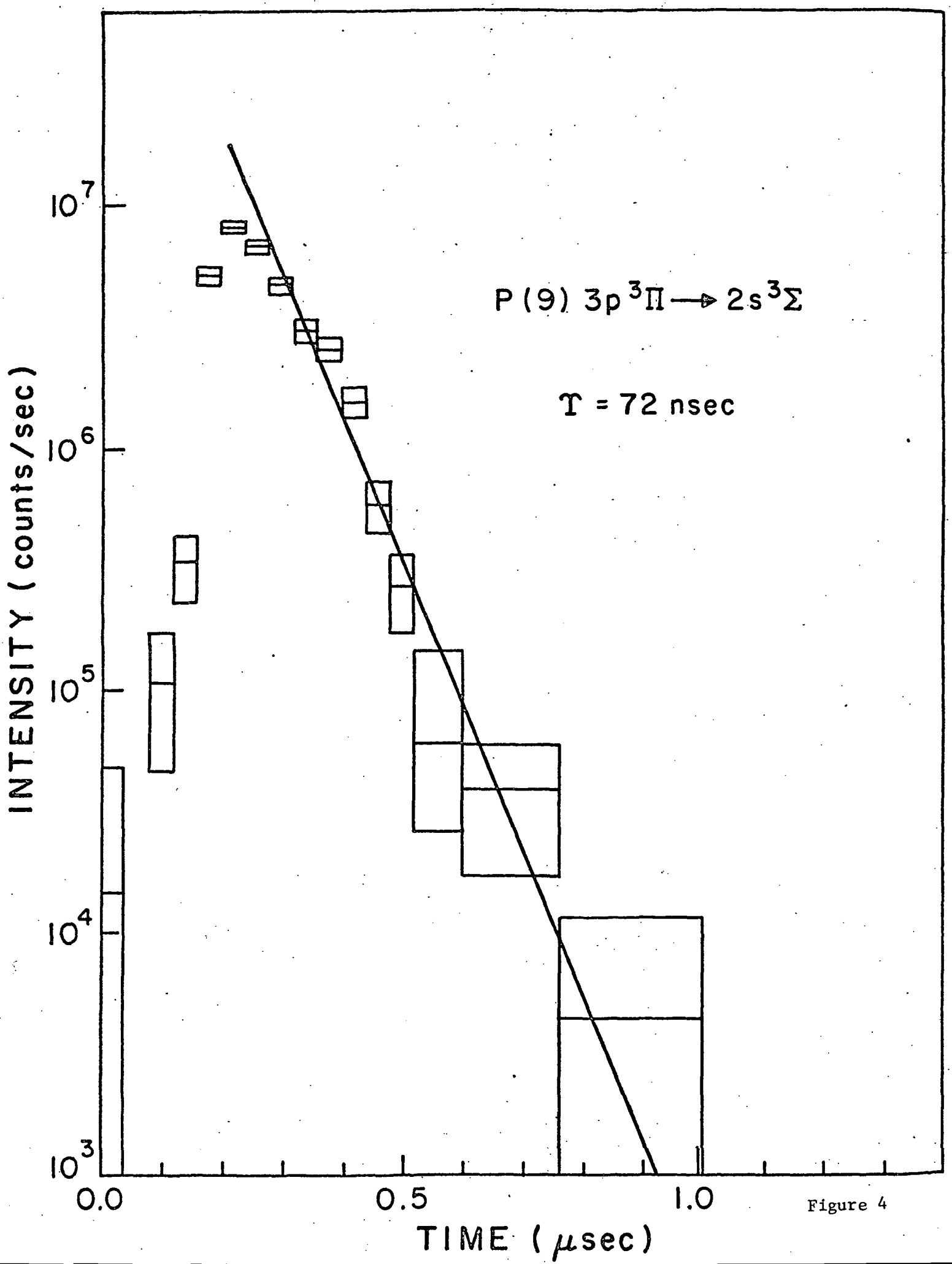
P(9) $3p\,^3\Pi \longrightarrow 2s\,^3\Sigma$
$\tau$ = 72 nsec
INTENSITY (counts/sec)
$10^7$
$10^6$
$10^5$
$10^4$
$10^3$
0.0
0.5
1.0
TIME ($\mu$sec)

Figure 4

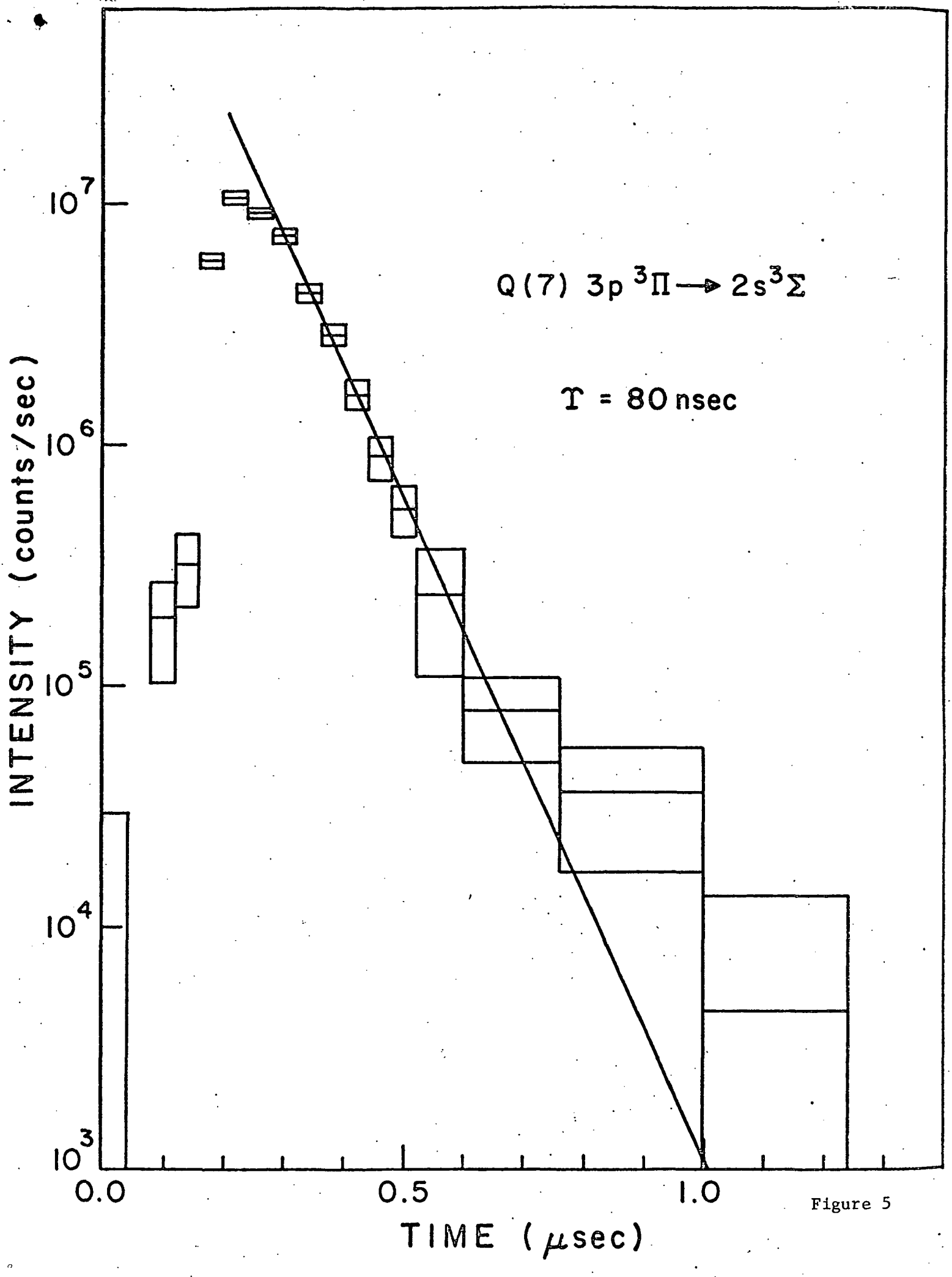
Q(7) 3p $^3\Pi \rightarrow 2s\,^3\Sigma$
$\tau$ = 80 nsec
INTENSITY (counts/sec)
$10^7$
$10^6$
$10^5$
$10^4$
$10^3$
0.0
0.5
1.0
TIME ($\mu$sec)

Figure 5